Cell Stem Cell
Article

Metformin Activates an Atypical PKC-CBP Pathway to Promote Neurogenesis and Enhance Spatial Memory Formation

Jing Wang,[1,2] Denis Gallagher,[1,2,4,9] Loren M. DeVito,[3,9] Gonzalo I. Cancino,[1,2] David Tsui,[1,5] Ling He,[8] Gordon M. Keller,[4] Paul W. Frankland,[3,5,6] David R. Kaplan,[2,5,7] and Freda D. Miller[1,4,5,6,7,*]
[1]Programs in Developmental and Stem Cell Biology
[2]Cell Biology
[3]Neurosciences and Mental Health
Hospital for Sick Children, Toronto, ON M5G 1X8, Canada
[4]McEwen Center for Regenerative Medicine, University Health Network, Toronto, ON M5G 1L7, Canada
[5]Institute of Medical Science
[6]Department of Physiology
[7]Department of Molecular Genetics
University of Toronto, Toronto, ON M5SG 1A8, Canada
[8]Department of Pediatrics and Medicine, Johns Hopkins Medical School, Baltimore, MD 21287, USA
[9]These authors contributed equally to this work
*Correspondence: fredam@sickkids.ca
DOI 10.1016/j.stem.2012.03.016

SUMMARY

Although endogenous recruitment of adult neural stem cells has been proposed as a therapeutic strategy, clinical approaches for achieving this are lacking. Here, we show that metformin, a widely used drug, promotes neurogenesis and enhances spatial memory formation. Specifically, we show that an atypical PKC-CBP pathway is essential for the normal genesis of neurons from neural precursors and that metformin activates this pathway to promote rodent and human neurogenesis in culture. Metformin also enhances neurogenesis in the adult mouse brain in a CBP-dependent fashion, and in so doing enhances spatial reversal learning in the water maze. Thus, metformin, by activating an aPKC-CBP pathway, recruits neural stem cells and enhances neural function, thereby providing a candidate pharmacological approach for nervous system therapy.

INTRODUCTION

Adult neural stem cells and the new neurons that they generate play key functional roles in the mammalian brain (Zhao et al., 2008). Intriguingly, growing evidence indicates that neural stem cells are also recruited in an attempt at endogenous repair in the injured or degenerating brain (Kernie and Parent, 2010), findings that suggest that if we could exogenously recruit adult neural stem cells, this might provide a novel therapeutic strategy. Some studies have attempted to do this with growth factors, but this approach has not been successful in part because of difficulties in delivering growth factors to the nervous system and in part because these are broadly active and highly potent biological entities (Miller and Kaplan, 2012).

One alternative to growth factors are small molecules that promote stem cell self-renewal and/or differentiation either as identified by high throughput screens (Li et al., 2012) or by defining relevant signaling pathways. With regard to the latter, we recently showed that the CBP transcriptional coactivator was necessary for optimal differentiation of embryonic neural precursors and that CBP ability to promote differentiation required phosphorylation by atypical protein kinase C (aPKC) (Wang et al., 2010). Intriguingly, in liver cells, the aPKC-CBP pathway is downstream of AMP kinase (AMPK) and is activated by the AMPK-activating drug metformin (He et al., 2009), which is widely used to treat type II diabetes and other metabolic syndromes. These findings therefore suggest that metformin might activate aPKCs in neural stem cells and, in so doing, allow their recruitment in the adult brain.

Here, we have tested this idea. We define distinct roles for aPKCs ι and ζ in regulating the neural precursor to neuron transition and show that aPKCζ regulates the genesis of neurons in a CBP-dependent fashion. Moreover, we show that metformin can activate this aPKC-CBP pathway to promote rodent and human neurogenesis in culture. Finally, we show that metformin has similar actions in the adult mouse CNS in vivo, acting to increase the genesis of neurons in the hippocampus in a CBP-dependent fashion and, in so doing, to enhance spatial reversal learning in a water maze task. Thus, metformin represents a candidate pharmacological approach for recruitment of neural stem cells in the adult human brain, a strategy that might be of therapeutic value for the injured or degenerating nervous system.

RESULTS

Atypical Protein Kinase C Isoforms Differentially Regulate the Radial Precursor to Neuron Transition during Embryonic Cortical Neurogenesis

We previously showed that two aPKC isoforms, ι and ζ, are expressed in the developing murine cortex and that aPKCζ is

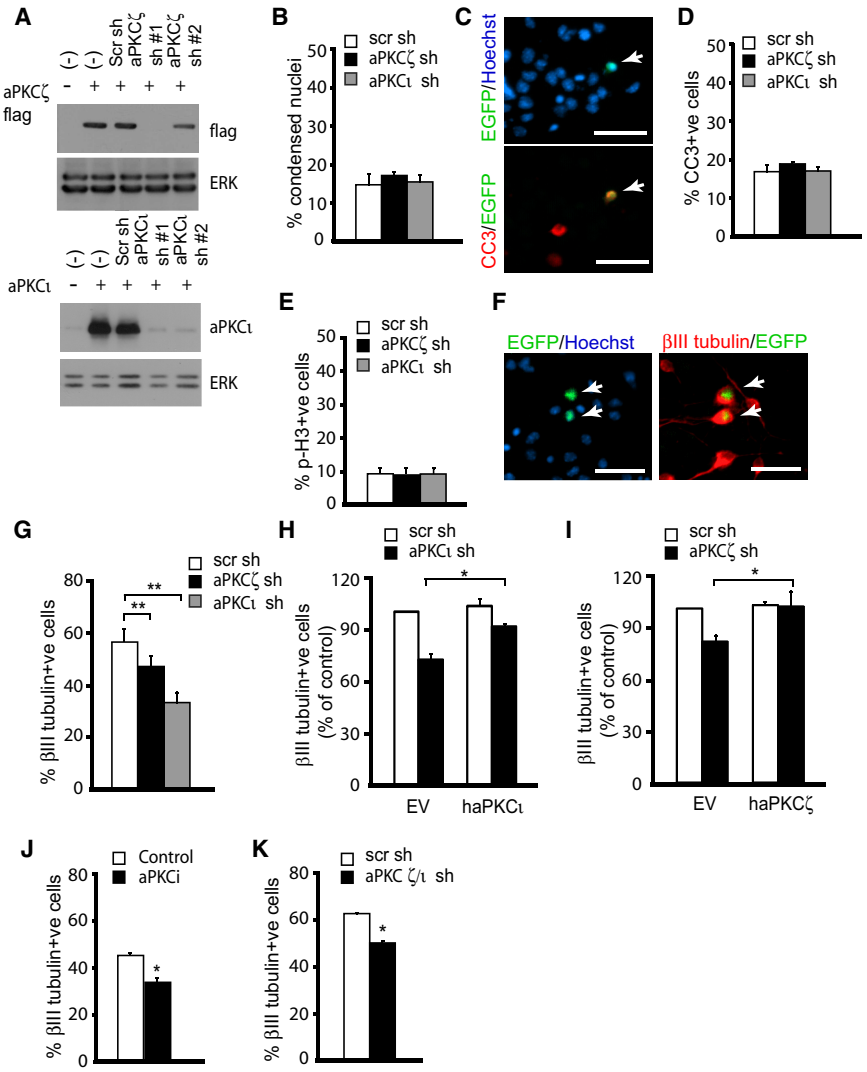

Figure 1. aPKCs ζ and ι Regulate Cortical Precursor Differentiation into Neurons in Culture

(A) Western blot analysis of HEK293 cells cotransfected with a flag-tagged expression construct for murine aPKCζ (top) or aPKCι (bottom) and either a scrambled shRNA (Scr) or one of two shRNAs specific for aPKCζ (top) or aPKCι (bottom). Blots were probed for the flag tag (top) or aPKCι (bottom) and reprobed for total ERK as a loading control.

(B–D) Precursors were cotransfected with plasmids encoding EGFP and aPKCζ, aPKCι, or scrambled shRNAs for 2 days, immunostained for EGFP (C, green) and cleaved caspase-3 (C, red), and counterstained with Hoechst 33258 (C, blue) and the percentage of transfected cells with condensed, apoptotic morphology (B) or expressing cleaved caspase-3 (CC3) (D) was determined. In (C) the same field is shown in both panels, and arrows denote a double-labeled cell with a condensed nucleus. $p > 0.05$; n = 3 independent experiments, pooled. Scale bars represent 25 μm.

(E) Percentage of transfected, phospho-histone H3-positive cells in cultures cotransfected with EGFP and aPKCζ, aPKCι, or scrambled shRNAs for 2 days. $p > 0.05$; n = 3 independent experiments, pooled.

(F) Precursors cotransfected with plasmids encoding EGFP and scrambled shRNA for 3 days, immunostained for EGFP (green) and βIII-tubulin (red), and counterstained with Hoechst 33258 (blue). The same field is shown in both panels, and arrows denote double-labeled cells. Scale bars represent 50 μm.

(G) Percentage of transfected, βIII-tubulin-positive cells in precursor cultures cotransfected with EGFP and aPKCζ, aPKCι or scrambled shRNAs for 3 days, as shown in (F). $^{**}p < 0.01$; n = 4–5 independent experiments, pooled.

(H and I) Percentage of βIII-tubulin-positive transfected neurons in precursor cultures 3 days after cotransfection with aPKCι (H) or aPKCζ (I) shRNA and expression plasmids for EGFP and human aPKCι (H) or aPKCζ (I). The number of transfected neurons under control conditions was normalized to 100%. $^{*}p < 0.05$; n = 3 independent experiments each, pooled.

(J) Percentage of βIII-tubulin-positive cells in precursor cultures treated with myristoylated aPKC pseudosubstrate peptide inhibitor (2 μM) or water, as a control, for 3 days. $^{*}p < 0.05$; n = 4 independent experiments, pooled.

(K) Percentage of transfected, βIII-tubulin-positive cells in precursors cotransfected with EGFP and aPKCζ plus aPKCι shRNAs, or with scrambled shRNA for 3 days, and analyzed as shown in (F). $^{*}p < 0.05$; n = 3 independent experiments, pooled.

Error bars represent SEM. See also Figure S1.

essential for the genesis of glial cells from cultured neural precursors (Wang et al., 2010). To ask whether aPKCs were also essential for neurogenesis, we studied cultured radial precursors from the E12.5 murine cortex that generate neurons first and glia second. We knocked down the aPKC isoforms in these precursors with previously characterized shRNAs (He et al., 2009; Wang et al., 2010), confirming their efficacy with two experiments. First, we cotransfected them individually into HEK293 cells along with aPKCι or ζ expression plasmids, as relevant; western blots confirmed that the shRNAs effectively knocked down aPKC isoform expression relative to either a scrambled shRNA or no shRNA (Figure 1A). Second, we cotransfected each shRNA with an EGFP expression plasmid into cultured cortical precursors and immunostained them 2 days later for aPKCι or ζ; the proportion of EGFP-positive cells expressing no or low aPKCι or ζ was increased by approximately 2-fold and 1.7-fold, respectively (Figures S1A and S1B available online).

We then used these shRNAs to ask what role aPKCs played in neural precursors. Cortical precursors were cotransfected with an EGFP plasmid and either aPKCζ shRNA#1 or aPKCι shRNA#1 and analyzed 3 days later when many precursors had differentiated into neurons. As a control, we used a scrambled shRNA that had no effect on cortical precursor biology (Figure S1C). Quantification of condensed, apoptotic nuclei (Figures 1B and 1C) and immunostaining for the apoptotic marker cleaved caspase-3 (Figures 1C and 1D) indicated that neither aPKC isoform was essential for cell survival. Similarly,

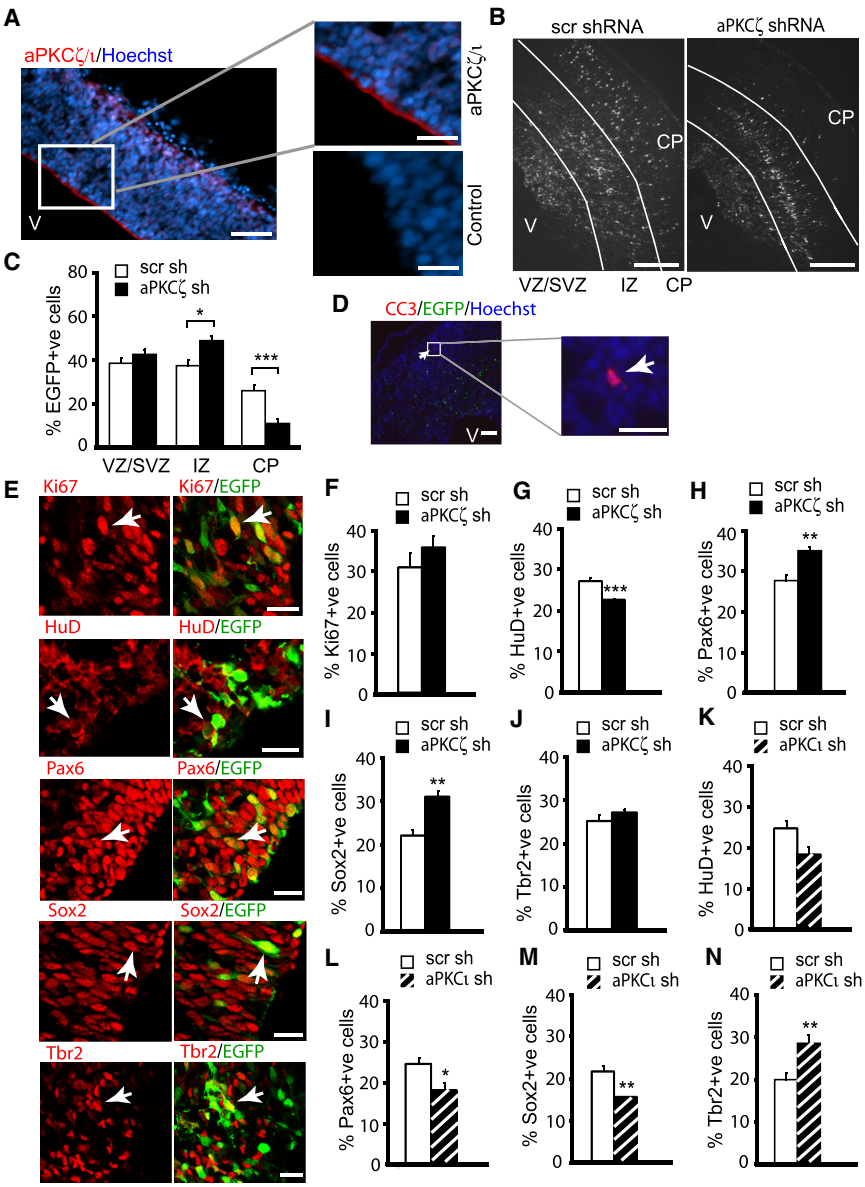

Figure 2. Genetic Knockdown of aPKCs Differentially Regulates Neural Precursor Differentiation In Vivo

(A) Immunostaining with an antibody for total aPKC (red; Hoechst 33258 counterstain is blue) on coronal E12 cortical sections. The boxed area is enlarged at right to show aPKC immunoreactivity adjacent to the ventricle (V). Control is immunostained with secondary antibody alone. Scale bars represent 50 μm (left) and 25 μm (right).

(B–N) E13/14 cortices were electroporated with plasmids encoding EGFP and aPKCζ (E–J), aPKCι (K–N), or scrambled shRNAs and sectioned coronally for analysis 3 days later.

(B) Immunostaining for EGFP (white) in sections electroporated with scrambled (left) or aPKCζ (right) shRNAs. White lines denote region boundaries. V denotes the ventricle. Scale bars represent 250 μm.

(C) Percentage of EGFP-positive cells within VZ/SVZ, IZ, and CP as shown in (B). *p < 0.05; ***p < 0.001; n = 4–6 brains each.

(D) Immunostaining for EGFP (green) and CC3 (red; blue is Hoechst 33258) in the section electroporated with scrambled shRNA. The boxed area at left is shown at higher magnification at right. Arrows denote a CC3-positive cell. V denotes the ventricle. Scale bars represent 100 μm (left) and 25 μm (right).

(E) Confocal images of cortical sections electroporated with aPKCζ shRNA (top) or scrambled shRNA (all other panels) and double-labeled for EGFP (green) and Ki67, HuD, Pax6, Sox2, or Tbr2, as indicated (all red). In all cases, the same field is shown in left and right panels, and the arrows denote double-labeled cells. All panels show the VZ/SVZ except for the HuD panel, which shows the CP. Scale bars represent 20 μm.

(F–J) Percentage of transfected Ki67-positive (F), HuD-positive (G), Pax6-positive (H), Sox2-positive (I), or Tbr2-positive (J) cells in cortices electroporated with aPKCζ or scrambled shRNAs and immunostained as in (E). **p < 0.01; ***p < 0.001; n = 4–6 brains each.

(K–N) Percentage of transfected, HuD-positive (K), Pax6-positive (L), Sox2-positive (M), or Tbr2-positive (N) cells in cortices electroporated with aPKCι or scrambled shRNAs and immunostained as in (E). *p < 0.05; **p < 0.01; n = 4–6 brains each. Error bars represent SEM. See also Figure S2.

immunostaining of transfected cultures for two markers of proliferating cells, phosphohistone H3 (Figure 1E) and Ki67 (Figure S1D), demonstrated that cell division was not altered by either shRNA. In contrast, both aPKC isoforms were necessary for neurogenesis; knockdown of either aPKCζ or aPKCι significantly decreased the proportion of βIII-tubulin-positive newly born neurons (Figures 1F and 1G).

We confirmed the specificity of this neurogenesis phenotype in three ways. First, we showed that aPKCι shRNA#2 and aPKCζ shRNA#2 also decreased neurogenesis without affecting proliferation (Figures S1E and S1F). Second, we rescued the decreased neurogenesis by coincidently expressing human aPKCι or ζ, which are not targeted by the murine shRNAs (Figures 1H and 1I). Third, we inhibited total aPKC activity by using a myristoylated aPKC pseudosubstrate peptide inhibitor that is efficacious in cortical precursors (Wang et al., 2010) and that blocks the activity of both isoforms. This inhibitor significantly reduced neurogenesis at 3 days (Figure 1J), and the magnitude of this decrease was similar to that seen when precursors were cotransfected with aPKCι and ζ shRNAs together (Figure 1K). Thus, aPKCs normally regulate cortical neurogenesis in culture.

We therefore asked whether aPKCs also regulate cortical neurogenesis in vivo; our previous biochemical analysis showed cortical expression of both aPKC isoforms from E12, the earliest time point examined, until birth (Wang et al., 2010). Immunostaining with a pan-aPKC antibody demonstrated that aPKCs were apically localized in precursors that line the ventricles in the E12 cortex (Figure 2A), as previously reported (Imai et al.,

2006; Costa et al., 2008), and consistent with an association between aPKCι and the apical polarity complex in radial precursors (Costa et al., 2008; Bultje et al., 2009). We therefore knocked down each aPKC isoform individually in radial precursors by in utero electroporation of the shRNAs together with a cytoplasmic EGFP expression plasmid into E13/14 cortices (Wang et al., 2010). This approach electroporates radial precursors that line the ventricle, many of which will then differentiate into neurons in the ventricular zone/subventricular zone (VZ/SVZ), prior to their migration through the intermediate zone (IZ) to the cortical plate (CP). At later time points the same precursor pool generates glial cells and adult neural stem cells.

Analysis of cortices 3 days postelectroporation demonstrated that both aPKC isoforms regulated the radial precursor to neuron transition but that they did so in different ways. For aPKCζ, analysis of the location of electroporated cells showed a decrease in EGFP-positive cells within the CP and a small increase in the IZ (Figures 2B and 2C). To ask about the cellular basis of this phenotype, we characterized the survival, proliferation and identity of the electroporated cells. Immunostaining for cleaved caspase-3 (Figure 2D) showed that survival was unaffected, with only five to ten positive cells per cortical section with or without aPKCζ knockdown. Immunostaining for Ki67 (Figure 2E) showed that the percentage of proliferating cells was also unchanged (Figure 2F). In contrast, immunostaining for the neuron-specific protein HuD demonstrated that aPKCζ knockdown reduced the number of EGFP-positive neurons (Figures 2E and 2G), thereby explaining the decrease in EGFP-positive cells in the CP. To ask whether undifferentiated precursors were coincidentally increased, we immunostained sections for the radial precursor markers Pax6 and Sox2 (Figure 2E); aPKCζ knockdown increased both populations (Figures 2H and 2I). In contrast, immunostaining for Tbr2, which marks the basal progenitor transit-amplifying cells in this system, showed that they were unaffected (Figures 2E and 2J). Thus, aPKCζ promotes differentiation of radial precursors into neurons in vivo.

A similar analysis for the aPKCι knockdown showed that it did not affect the distribution of EGFP-positive transfected cells (Figures S2A and S2B), nor did it affect cleaved caspase-3-positive cells. There was also no significant change in HuD-positive electroporated neurons, although there was a trend toward a decrease (Figure 2K). In contrast, aPKCι knockdown significantly altered precursor populations. Pax6-positive and Sox2-positive radial precursors were decreased (Figures 2L and 2M), and Tbr2-positive basal progenitors were correspondingly increased (Figure 2N). Thus, aPKCι functions to maintain radial precursors and to inhibit their transition to basal progenitors, consistent with its role in the polarity complex.

These data argue that aPKCs ζ and ι control cortical neurogenesis via distinct mechanisms. In this regard, we previously showed that aPKCζ but not ι regulated cortical gliogenesis by phosphorylating and activating CBP (Wang et al., 2010). We confirmed this previous result (Figures S1G and S1H) and then determined whether CBP was also downstream of aPKCζ with regard to neurogenesis. We did this genetically, asking whether a CBP phosphomimic that was mutated at the aPKC phosphorylation site could rescue the decrease in neurogenesis caused by aPKCζ knockdown. For comparison, we examined aPKCι knockdown. Quantification of cotransfected precursor cultures showed that the CBP phosphomimic rescued the decreased neurogenesis seen with aPKCζ but not aPKCι knockdown (Figure 3A). Thus, aPKCζ enhances neurogenesis by activating CBP.

Metformin Activates Atypical PKC and Promotes Neurogenesis in Rodent Cortical Precursors

Our data indicate that the aPKC-CBP pathway promotes neurogenesis. Because metformin activates this pathway in liver cells (He et al., 2009), we asked whether it would also do so in cortical precursors. Precursors were cultured for 1 day and exposed to 15 mM metformin for 15 min, and lysates were probed with antibodies for total aPKC and for aPKC phosphorylated at threonine 403, which is critical for kinase activity (Messerschmidt et al., 2005). Metformin caused a modest but reproducible increase in aPKC threonine 403/410 phosphorylation (Figure 3B). We then cultured precursors in 500 μM metformin and asked how this affected their biology. Analysis of cleaved caspase-3 and cells with condensed nuclei at 2 days showed that cell survival was unaffected by metformin (Figures 3C and 3D). Similarly, cell division, as monitored by phosphohistone H3-positive cells at 2 days, was unchanged (Figure 3E). In contrast, metformin almost doubled the percentage of βIII-tubulin-positive neurons present at 3 days (Figures 3F and 3G), an increase that was accompanied by a corresponding decrease in the proportion of Pax6-positive (Figure 3H) and Sox2-positive (Figure 3I) precursors.

We next asked whether the metformin-induced increase in neurogenesis required the aPKC-CBP pathway. Initially, we asked about the aPKCs, transfecting precursors with shRNAs for both isoforms at levels that did not significantly decrease basal neurogenesis (Figure 3J), presumably because the remaining aPKC levels were sufficient for maintenance. We then cultured these transfected precursors with or without metformin. Analysis of transfected βIII-tubulin-positive neurons after 3 days (Figure 3J) showed that metformin increased neurogenesis and that the aPKC shRNAs inhibited metformin-induced neurogenesis. We then asked about CBP, by using previously characterized siRNAs (Wang et al., 2010). Precursors were transfected with CBP or scrambled siRNA and were cultured in metformin for 3 days. CBP knockdown completely inhibited the metformin-induced increase in neurogenesis (Figure 3K).

These results indicate that metformin activates the aPKC-CBP pathway in cortical precursors, thereby enhancing neurogenesis. We therefore asked whether it also promotes gliogenesis, as would be predicted by our previous results (Wang et al., 2010). To do this, we added metformin to precursor cultures on day 2 and analyzed them on day 7, when endogenous gliogenesis has commenced. Metformin increased genesis of both GFAP-positive astrocytes and A2B5-positive oligodendrocyte precursors (Figure 3L), suggesting that metformin activates an aPKC-CBP pathway to generally promote cortical precursor differentiation.

Finally, we asked whether metformin affected cortical precursor differentiation in vivo by electroporating E13/14 embryos with an EGFP expression construct and by treating their mothers with metformin daily for 4 days, starting 1 day prior to electroporation. Analysis 3 days postelectroporation showed that the location of EGFP-positive cells was similar in progeny of control versus metformin-treated mothers (Figures S3A and S3B).

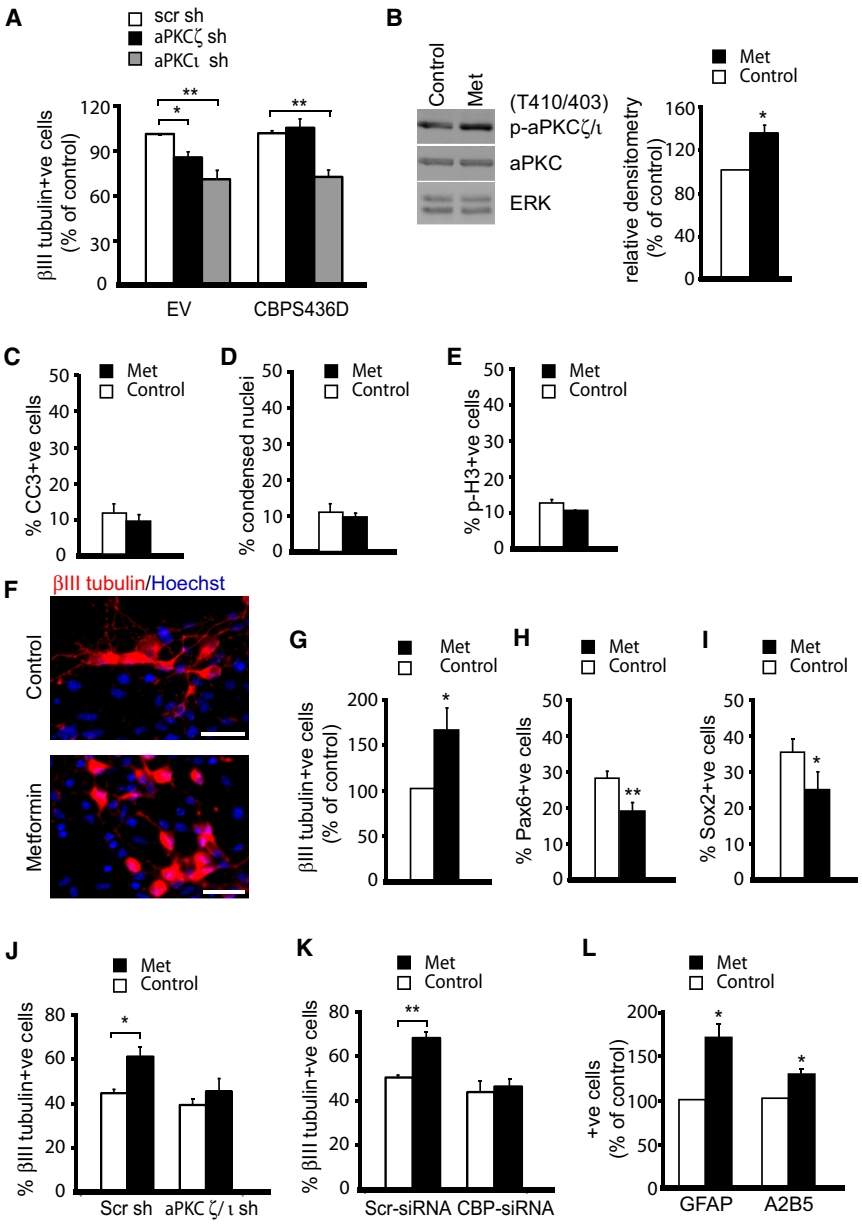

Figure 3. Metformin Activates an aPKC-CBP Pathway to Promote Genesis of Neurons from Murine Cortical Precursors

(A) Percentage of transfected, βIII-tubulin-positive cells in precursor cultures 3 days after cotransfection with EGFP and aPKCζ, aPKCι, or scrambled shRNAs plus or minus a CBP phosphomimic. The number of neurons generated with the scrambled shRNA was normalized to 100%. *$p < 0.05$; **$p < 0.01$; n = 3 independent experiments.

(B) Western blot for aPKC ζ/ι phosphorylation at T410/403 in cortical precursors treated with water (as a control) or metformin (15 mM) for 15 min. Blot was reprobed for total aPKC and for ERKs as a loading control. The graph shows the relative level of phosphorylation of aPKC normalized to total aPKC, as determined by densitometry. *$p < 0.05$; n = 3 independent experiments.

(C–I) Cultured cortical precursors were treated with 500 μM metformin (Met) or water (Control) for 2 (C–E) or 3 (F–I) days.

(C and D) Percentage of transfected cells that were positive for cleaved caspase-3 (CC3) (C) or that displayed condensed, apoptotic nuclei (D). $p > 0.05$; n = 3 independent experiments, pooled.

(E) Percentage of cells positive for the proliferation marker phospho-histone H3. $p > 0.05$; n = 3 independent experiments, pooled.

(F) Immunostaining (red; blue is Hoechst 33258 to show nuclei) for βIII-tubulin in precursor cultures treated with water or metformin for 3 days. Scale bars represent 25 μm.

(G) Percentage of βIII-tubulin-positive neurons in precursor cultures as shown in (F), where the number of neurons under control conditions was normalized to 100%. *$p < 0.05$; n = 5 independent experiments, pooled.

(H and I) Percentage of Pax6-positive precursors (H) or Sox2-positive precursors (I) in cultures treated as in (F). *$p < 0.05$; **$p < 0.01$; n = 4 independent experiments, pooled.

(J and K) Percentage of βIII-tubulin-positive neurons in cultures treated for 2 days with 500 μM metformin or water (Control) 18 hr after cotransfection with EGFP and either (J) aPKCζ plus aPKCι shRNAs or (K) CBP siRNAs. As controls, cells were cotransfected with scrambled shRNA or siRNA. In (J), only half as much aPKC shRNA was used as in Figure 1K. *$p < 0.05$; **$p < 0.01$; n = 3 (J) or 4 (K) independent experiments, pooled.

(L) Percentage of GFAP-positive and A2B5-positive cells in precursor cultures treated with water or 500 μM metformin from day 2 to day 7, where the numbers of astrocytes or oligodendrocyte precursors under control conditions were normalized to 100%. *$p < 0.05$; n = 3 independent experiments, pooled.

Error bars represent SEM. See also Figure S3.

Although the proportion of Pax6-positive precursors was unchanged (Figure S3D), there was a small but significant increase in HuD-positive neurons (Figure S3C), consistent with the culture data.

Metformin Enhances Neurogenesis from Human ESC-Derived Neural Precursors

If metformin could promote neurogenesis from human neural stem cells as it does from murine, then this might serve as the basis for a potential therapeutic strategy. To address this possibility, we developed a method for generating forebrain neural precursors from human embryonic stem cells (hESCs). Embryoid bodies (EBs) were generated from hESCs and were treated for 12 days with Dorsomorphin, an inhibitor of BMP signaling, and SB43152, an inhibitor of Lefty/Activin/TGF-β signaling (Chambers et al., 2009; Zhou et al., 2010). These differentiated EBs were dissociated and adhered to a laminin-coated surface. Immunostaining showed that approximately 60%–70% of the freshly plated cells expressed Pax6 (Figure 4A). In addition, they expressed other markers consistent with a forebrain precursor identity including nestin (Figure 4B), the radial precursor marker BLBP (data not shown), and the cortical marker Emx1

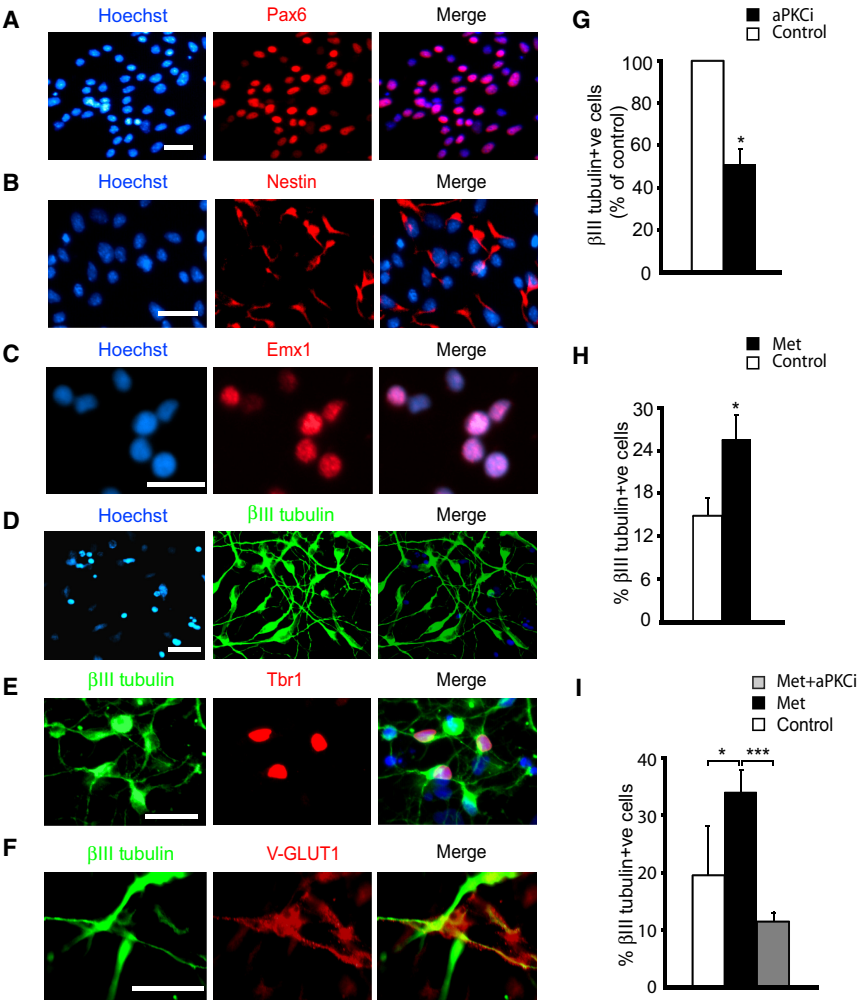

Figure 4. Metformin Activates aPKCs to Enhance the Genesis of Neurons from hESC-Derived Forebrain Neural Precursors

(A–C) hESCs were cultured as embryoid bodies in the presence of 2 μM Dorsomorphin and 10 μM SB43152 for 12 days, plated, and immunostained for Pax6 (A), nestin (B), and Emx1 (C) (all red; blue is Hoechst 33258). Scale bars represent 50 μm.

(D–F) Cells were cultured adherently for a further 10 days and immunostained for βIII-tubulin (D) and Tbr1 (E) or V-GLUT1 (F). Scale bars represent 50 μm.

(G–I) Neuralized embryoid bodies were plated with and without 2 μM aPKC pseudosubstrate inhibitor peptide (G), with and without 500 μM metformin (H), or with 500 μM metformin plus or minus the aPKC inhibitor (I) for 4 days, immunostained for βIII-tubulin, counterstained for Hoechst 33258, and the relative proportion of βIII-tubulin-positive neurons was determined. In (G), numbers of control neurons in each experiment were normalized to 100%. *$p < 0.05$, ***$p < 0.001$; n = 3 independent experiments.

Error bars represent SEM.

(Figure 4C). To ask whether these precursors would generate neurons, we differentiated them for 10 days in neural induction medium (see Experimental Procedures). Immunostaining showed that the Pax6-positive cells were replaced by morphologically complex glutamatergic neurons that expressed βIII-tubulin (Figure 4D), the glutamatergic neuron marker VGLUT1 (Figure 4F), and the cortical neuron marker Tbr1 (Figure 4E). Thus, as reported for murine ESCs (Bibel et al., 2007), in the absence of specific inductive signals, neuralized hESCs make forebrain radial precursors that generate glutamatergic neurons.

To ask whether aPKCs were important for human neurogenesis, we cultured dissociated hESC-derived neural precursors with or without the myristoylated aPKC peptide inhibitor for 4 days. This inhibitor had no effect on total cell number (quantified as cells/field; $p > 0.05$), but it decreased βIII-tubulin-positive neurons by almost 2-fold (Figure 4G). We then asked whether metformin enhanced neurogenesis by activating aPKC in human forebrain precursors. Cells were grown for 4 days with or without metformin plus or minus the myristoylated aPKC inhibitory peptide. This analysis showed that 500 μM metformin significantly increased βIII-tubulin-positive newly born neurons (Figure 4H) and that inhibition of the aPKCs abolished this increase (Figure 4I). Thus, as seen with murine precursors, metformin acts via aPKCs to promote human neurogenesis in culture.

Metformin Promotes Neurogenesis from Adult Forebrain Neural Precursors

To determine whether metformin also regulates adult neurogenesis, we studied neural precursor cells (NPCs) in the lateral ventricle SVZ, because some of these derive from embryonic cortical precursors (Merkle et al., 2004). Initially, we confirmed that forebrain NPCs express aPKCs, taking advantage of the fact that they will expand as neurospheres in culture. Immunostaining of primary SVZ neurospheres showed that most cells displayed aPKC immunoreactivity in both the cytoplasm and nucleus (Figure 5A). We confirmed that this was also true in vivo by immunostaining coronal sections through the adult cortex. Detectable aPKC immunoreactivity was seen in many neurons and white matter tracts, as previously reported (Naik et al., 2000; Oster et al., 2004) and was also observed in GFAP-positive cells within the SVZ (Figures S4A and S4B), probably type B NPCs.

Forebrain NPCs normally generate interneurons for the olfactory bulb. We therefore asked whether metformin increased olfactory neurogenesis; adult mice were injected with BrdU five times at 3 hr intervals to label dividing cells and were then treated with 200 mg/kg metformin daily for 21 days. Immunostaining of serial sections through the main olfactory bulbs of these mice (Figure 5B) showed that metformin significantly increased the number of BrdU-positive, NeuN-positive olfactory neurons in the granule cell layer (Figure 5C). We then asked whether metformin had any impact on the number of SVZ NPCs. Mice were injected with metformin daily for 7 days and coinjected with

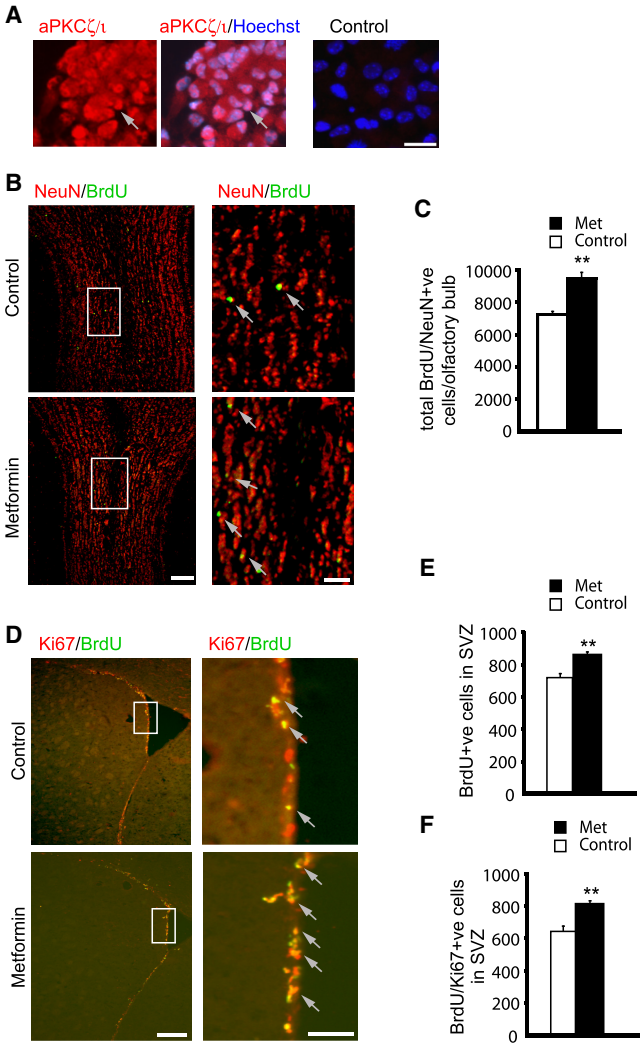

Figure 5. Metformin Promotes Neurogenesis in the Adult Murine Olfactory Bulb

(A) Primary passage adult SVZ neurospheres immunostained for total aPKCs (red; blue is Hoechst 33258). Control was immunostained with normal rabbit IgG and the same secondary antibody. Arrows denote aPKC-positive cells. Scale bar represents 20 μm.

(B) Immunostaining for BrdU (green) and NeuN (red) in coronal sections through the main olfactory bulb of mice injected with BrdU five times at 3 hr intervals and treated with 200 mg/kg metformin or PBS (Control) daily for 21 days. Right panels are higher magnifications of the boxed areas. Arrows denote double-labeled cells. Scale bars represent 200 μm (left) and 50 μm (right).

(C) Total number of BrdU-positive, NeuN-positive newborn neurons in control versus metformin-treated olfactory bulbs as determined from sections similar to those in (B). $^{**}p < 0.01$; n = 5 animals each.

(D) Immunostaining for BrdU (green) and Ki67(red) in coronal SVZ sections of mice injected with 200 mg/kg metformin or PBS (Control) daily for 7 days, and coinjected with BrdU on the seventh day, 24 hr prior to analysis. Right panels show higher magnifications of the boxed areas. Arrows denote double-labeled cells. Scale bars represent 200 μm (left) and 50 μm (right).

(E and F) Quantification of BrdU-positive (E) or BrdU and Ki67 double-positive (F) cells in the SVZ of control versus metformin-treated animals, determined from four anatomically matched coronal sections similar to those shown in (D). $^{**}p < 0.01$; n = 5 animals each.

Error bars represent SEM. See also Figure S4.

100 mg/kg BrdU on the final day. Analysis of coronal forebrain sections 24 hr later demonstrated that metformin significantly enhanced the number of BrdU-labeled cells (Figures 5D and 5E) and the number of cells double-labeled for BrdU and Ki67 (Figures 5D and 5F) over this time frame. Thus, metformin enhanced adult forebrain neurogenesis.

Metformin Enhances Hippocampal Neurogenesis in a CBP-Dependent Fashion

Because metformin enhanced the genesis of olfactory neurons, we asked whether it also increased adult hippocampal dentate gyrus neurogenesis. Immunostaining of hippocampal sections showed that aPKCs were detectably expressed in most dentate gyrus cells (Figure S4C) including some GFAP-positive cells within the subgranular zone (SGZ; Figure 6A), probably adult NPCs. We therefore asked whether metformin enhanced hippocampal neurogenesis; adult mice were injected daily with metformin and BrdU for 3 days, and then were injected with metformin alone for 9 additional days. Immunostaining of hippocampal sections (Figure 6B) demonstrated that metformin significantly increased the number of BrdU-positive, NeuN-positive newly born granule neurons by approximately 30% (Figure 6C). Consistent with this, we observed an increase in cells expressing doublecortin, a marker of newborn neurons (Figures 6D and 6E). Thus, metformin enhanced adult hippocampal neurogenesis.

We also asked whether metformin had an impact on the hippocampal NPC pool, immunostaining sections from the same experiments for BrdU and for GFAP, which is expressed in SGZ NPCs and in astrocytes in the hilus. This analysis showed that metformin did not significantly change GFAP-positive, BrdU-positive NPCs in the SGZ (Figure 6F). It also showed that virtually all of the GFAP-positive, BrdU-positive cells were located in the SGZ, with very few double-labeled hilar astrocytes in either controls or metformin-treated animals (an average of two versus seven cells/dentate gyrus in control versus metformin-treated mice). We did not detect BrdU-positive cells coexpressing the oligodendrocyte marker GalC in either control or metformin-treated hippocampi. To confirm that metformin did not alter NPC pools, we injected mice with metformin daily for 7 days and coinjected them with BrdU on the final day (Figure 6G). Immunostaining of serial sections showed that this treatment did not alter the number of proliferating BrdU- and Ki67-positive cells (Figure 6H).

Our culture data indicate that metformin promotes neurogenesis via an aPKC-CBP pathway. To ask whether the same pathway is important in vivo, we used mice that are heterozygous for CBP (Kung et al., 2000). Previous work indicates that the adult brain in $cbp^{+/-}$ mice is morphologically normal (Alarcón et al., 2004; Wang et al., 2010), as is basal hippocampal neurogenesis (Lopez-Atalaya et al., 2011). We first confirmed this latter finding by administering BrdU for 3 days to 2-month-old $cbp^{+/+}$ and $cbp^{+/-}$ littermates. Quantification of BrdU/NeuN-positive newborn neurons 9 days later showed that basal hippocampal neurogenesis was similar in mice of both genotypes (Figure 6J), as reported (Lopez-Atalaya et al., 2011). We then asked whether metformin required normal levels of CBP to enhance hippocampal neurogenesis. Seven-month-old $cbp^{+/+}$ and $cbp^{+/-}$ littermates were treated with metformin and BrdU for

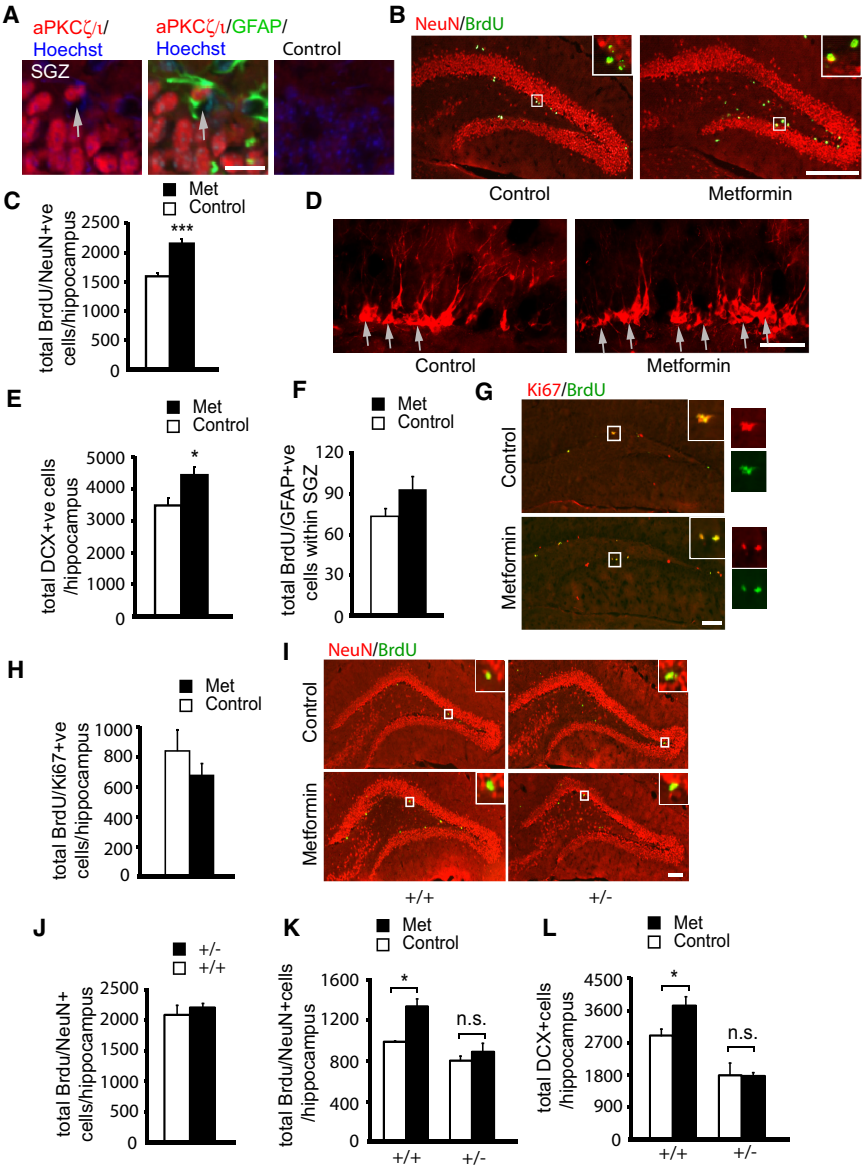

Figure 6. Metformin Promotes Neurogenesis in the Adult Murine Hippocampus in a CBP-Dependent Fashion

(A) Confocal image of a coronal adult dentate gyrus section immunostained for total aPKC (red) and GFAP (green). Arrows denote a double-labeled cell in the SGZ. The control was immunostained with normal rabbit IgG and the same secondary antibody. Scale bar represents 20 μm.

(B) Coronal hippocampal dentate gyrus sections from mice injected with metformin or PBS (control) daily for 12 days, with BrdU coinjection for the first 3 days. Sections were immunostained for BrdU (green) and NeuN (red), and insets show higher magnifications of the boxed areas. Scale bar represents 200 μm.

(C) Total number of BrdU-positive, NeuN-positive newborn neurons in PBS (Control)- versus metformin (Met)-treated hippocampi determined from sections as in (B). ***$p < 0.001$; $n = 9$ animals each.

(D) Hippocampal dentate gyrus coronal sections from adult mice treated as in (B) and immunostained for doublecortin (DCX). Arrows denote positive cells. Scale bar represents 50 μm.

(E) Total number of doublecortin-positive neurons in PBS (Control)- versus metformin (Met)-treated hippocampi determined from sections as in (D). *$p < 0.05$; $n = 9$ animals each.

(F) Total number of BrdU-positive, GFAP-positive cells within the SGZ of PBS (Control)- versus metformin (Met)-treated hippocampi determined from sections similar to those in (B) that were immunostained for GFAP rather than NeuN. $p > 0.05$; $n = 5$ animals each.

(G) Immunostaining for BrdU (green) and Ki67 (red) in coronal dentate gyrus sections of mice injected with PBS (Control) or metformin (Met) daily for 7 days and coinjected with BrdU on the last day. The insets show the boxed areas at higher magnification. Scale bar represents 100 μm.

(H) Total number of BrdU and Ki67 double-positive cells in the SGZ of PBS (Control) and metformin (Met)-treated mice, determined from sections as in (G). $p > 0.05$; $n = 5$ animals each.

(I) Coronal dentate gyrus sections of 7-month-old $cbp^{+/+}$ and $cbp^{+/-}$ mice injected with metformin or PBS (control) daily for 12 days, with BrdU coinjection for the first 3 days. Sections were immunostained for BrdU (green) and NeuN (red). The insets show the boxed areas at higher magnification. Scale bar represents 200 μm.

(J) Total number of BrdU-positive, NeuN-positive newborn neurons in hippocampi of 2-month-old $cbp^{+/+}$ versus $cbp^{+/-}$ littermates. Mice were injected with BrdU for 3 consecutive days and analyzed as in (I) 9 days later ($n = 4$ animals each, $p > 0.05$).

(K and L) Total number of BrdU-positive, NeuN-positive (K), and doublecortin-positive (L) newborn neurons in PBS (Control)- versus metformin (Met)-treated $cbp^{+/+}$ versus $cbp^{+/-}$ hippocampi from 7-month-old mice, determined from sections as in (I) and (D). *$p < 0.05$; $n = 4$–5 animals each.

Error bars represent SEM.

3 days and then metformin alone every day for 9 additional days. Immunostaining (Figure 6I) showed that although basal neurogenesis was decreased at this age, metformin still enhanced hippocampal neurogenesis in the wild-type $cbp^{+/+}$ mice (Figure 6K). In contrast, metformin did not enhance neurogenesis in mice that were haploinsufficient for CBP (Figure 6K). This conclusion was confirmed by quantifying doublecortin-positive newly born neurons in these hippocampi (Figure 6L). Thus, metformin promotes neurogenesis by activating an aPKC-CBP pathway both in culture and in vivo.

Metformin Enhances Spatial Memory Formation

Adult neurogenesis in the hippocampus plays a key role in spatial memory function, regulating acquisition of a spatial memory and subsequent flexible use of that spatial memory (Dupret et al., 2007; Garthe et al., 2009; Stone et al., 2011). We therefore developed a hidden platform version of the water maze task where mice were asked to acquire an initial platform location and then to rapidly learn a second platform location (Figure 7A). To determine whether metformin had any effect on learning in this paradigm, we injected adult mice with metformin (200 mg/kg)

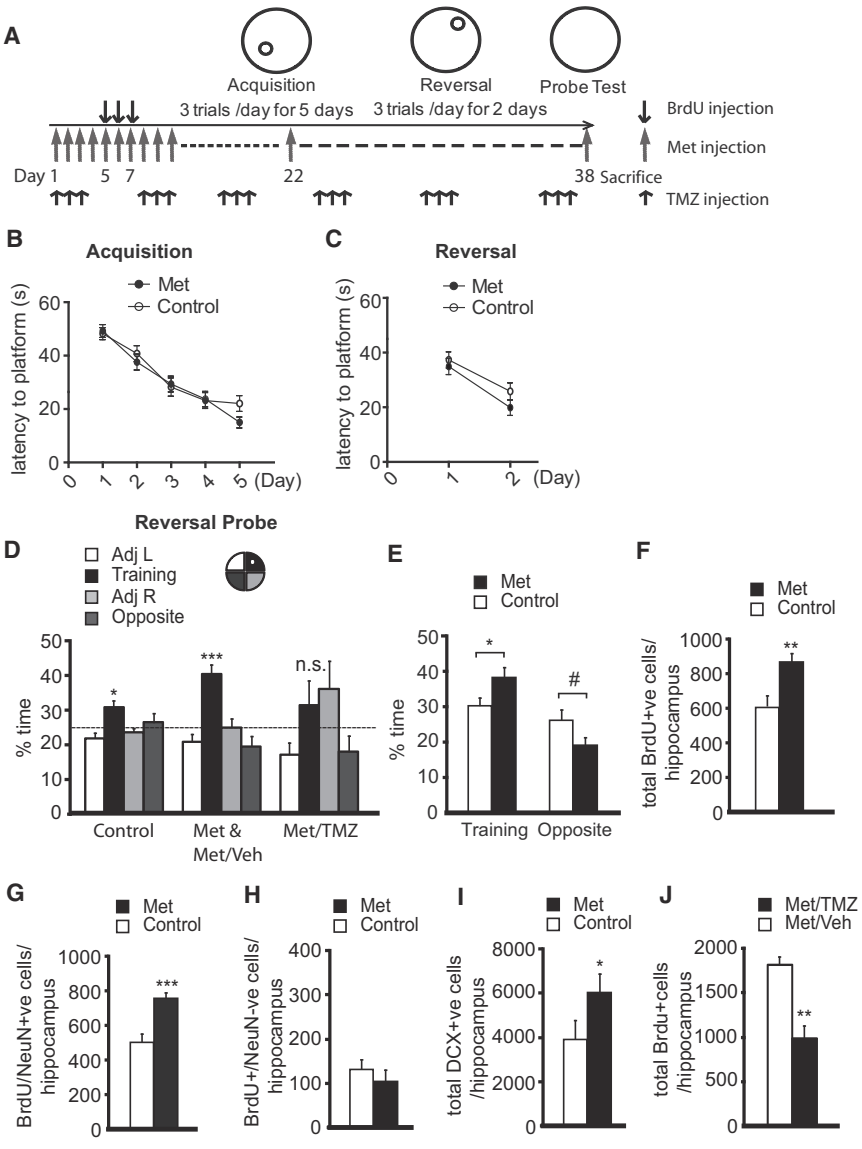

Figure 7. Metformin Treatment Enhances Spatial Memory Formation in Adult Mice

(A) Schematic of the BrdU, metformin, and TMZ injections relative to the time course of training and testing protocols for the Morris water maze experiments. Metformin or sterile saline (as a control) were injected daily for the 38 day period and a subset of mice were coinjected with BrdU as indicated. Some mice also received injections of TMZ or vehicle at the indicated time points.

(B) Acquisition of the initial platform location across 5 days of training with latency to reach the platform as a measurement of learning. Metformin and control groups were similar in the initial acquisition of the task (2-way ANOVA: group $F_{(1,279)} = 0.662$, $p = 0.42$; training day $F_{(1,279)} = 34.311$, $p < 0.001$; group X training day interaction $F_{(4,279)} = 0.734$, $p = 0.57$; $n = 56$).

(C) Acquisition of the platform location after it was moved to the opposite quadrant of the pool. Both metformin and control groups acquired the new location at equivalent rates (2-way ANOVA: group $F_{(1,111)} = 1.752$, $p = 0.19$; training day $F_{(1,111)} = 17.727$, $p < 0.001$; group X training day interaction $F_{(1,111)} = 0.325$, $p = 0.57$; $n = 56$).

(D) After acquisition of the new location, the platform was removed and mice were given a 60 s probe trial. Both the control and the combined metformin- and metformin/vehicle-treated groups showed significant differences between the time spent in the different quadrants by one-way ANOVA. Post-hoc analysis showed that the metformin/metformin plus vehicle-treated mice searched selectively in the target quadrant relative to all the other quadrants (one-way ANOVA, $F_{(3,111)} = 11.6$, $^{***}p < 0.0001$; training quadrant > all other quadrants, $p < 0.05$; $n = 14$ each of metformin and metformin plus vehicle, combined because they were not significantly different) while the control mice only searched significantly more in the target quadrant relative to the adjacent left quadrant (one-way ANOVA, $F_{(3,111)} = 3.202$, $^{*}p = 0.02$; training quadrant > adj l quadrant, $p < 0.05$; $n = 28$). In contrast to these two groups, the Met/TMZ group showed no significant preference for the training quadrant relative to the other three quadrants (one-way ANOVA, $F_{(3,51)} = 2.4$, $p = 0.07$; for the training quadrant relative to all other quadrants, n.s. $p > 0.05$; $n = 13$).

(E) Relative to control mice, the metformin-treated mice also spent a significantly greater amount of time searching in the quadrant containing the new platform location ($t_{(55)} = 4.277$, $p = .04$; $n = 28$ in each group) and significantly less time in the opposite quadrant where the target had been previously located ($t_{(55)} = 4.036$, $p = 0.05$; $n = 28$ in each group).

(F–H) Coronal dentate gyrus sections of mice treated with metformin or sterile saline (Control) as in (A) and injected with BrdU at the start of the experiment were analyzed anatomically by immunostaining for BrdU and NeuN (as in Figure 6B), and these sections were quantified for the total number of BrdU-positive cells (F), newly born BrdU-positive, NeuN-positive neurons (G), and BrdU-positive, NeuN-negative cells (H). $^{**}p < 0.01$, $^{***}p < 0.001$; $n = 5$ animals each.

(I) Coronal dentate gyrus sections similar to those in (F)–(H) were analyzed by immunostaining for doublecortin (as in Figure 6D), and these sections were quantified for the total number of doublecortin-positive neurons. $^{*}p < 0.05$; $n = 5$ animals each.

(J) Mice treated with metformin plus vehicle or metformin plus TMZ as in (A) were injected with BrdU at day 38 and coronal dentate gyrus sections were analyzed 1 day later by immunostaining for BrdU. The graph shows quantification of the number of BrdU-positive proliferating cells in these sections. $^{**}p < 0.01$; $n = 5$ animals each.

Error bars represent SEM. See also Figure S5.

or control (sterile saline) daily for 38 days, coinjecting some animals with BrdU on days 5, 6, and 7 to assess neurogenesis. From 22 to 38 days, mice were trained and assessed in this water maze task (Figure 7A). Metformin did not affect body weight over this time course (Figure S5A). Behavioral analysis showed that the metformin and control groups were similar in their acquisition of the initial platform location (Figure 7B) and that this initial spatial memory was stable in both groups, as assessed by probe tests 1 day and 1 week after completion of training (data not shown). Mice were then assessed on their ability to learn the

new platform location in the reversal phase of this task. Both groups were similar with regard to their rate of learning (Figure 7C), and both spent significantly longer in the target zone than in the other zones (Figure 7D). However, during the probe test, the metformin-treated mice spent significantly more time in the quadrant containing the new target (Figure 7E) while the control mice spent more time in the quadrant that had contained the platform in the initial training phase (the opposite quadrant) (Figure 7E). Both groups spent a similar amount of time in quadrants that had never contained either target (Figure 7D). Importantly, there was no difference between the two groups in the distance traveled (Figure S5B) or swimming speed (Figure S5C). Thus, metformin treatment selectively enhanced the ability to update spatial memory, consistent with previous studies demonstrating that neurogenesis is necessary for flexible memory processes (Dupret et al., 2007; Garthe et al., 2009).

We then analyzed a subset of these animals anatomically to ask whether the enhanced spatial memory formation was coincident with a long-term increase in dentate gyrus neurons. Immunostaining demonstrated that 1 month after BrdU injection, at the completion of behavioral training, the large majority of the BrdU-positive cells in the dentate gyrus were NeuN-positive neurons (compare Figures 7F and 7G). Moreover, the total number of BrdU-positive cells was increased by the metformin treatment (Figure 7F) as was the total number of BrdU-positive, NeuN-positive neurons (Figure 7G). In contrast, the number of BrdU-positive, NeuN-negative cells (presumably primarily NPCs) was unaltered (Figure 7H). Consistent with these findings, the number of doublecortin-positive cells was also increased (Figure 7I). Thus, metformin promotes the genesis of new hippocampal neurons and these neurons survive in the long term.

These results demonstrate a correlation between a metformin-induced increase in hippocampal neurogenesis and enhanced spatial learning. To ask whether this was a causal relationship, we took advantage of the fact that the only rapidly proliferating cells in the brain are NPCs. We therefore used the drug temozolomide (TMZ), a DNA alkylating agent that selectively induces the death of replicating cells, to decrease NPC numbers and ask whether this inhibited the metformin-induced increase in spatial memory. We and others have previously used this approach in adult neurogenesis studies (Garthe et al., 2009; Stone et al., 2011). To perform these experiments, we used the same metformin administration and training regimen but injected mice with 25 mg/kg TMZ for 6 cycles of 3 days on and 4 days off, starting from the first day of metformin injection throughout the training regimen (Figure 7A). As controls, mice were treated in the same way but were injected with vehicle rather than TMZ. Both of these groups were able to acquire the initial platform location in the water maze, and this initial memory was stable, as indicated by probe tests 1 day and 1 week later (Figures S5D and S5E). Analysis of the reversal phase of the water maze task demonstrated that the performance of metformin/vehicle-treated mice was similar to mice treated with metformin alone ($p > 0.05$). In contrast, mice treated with metformin and TMZ were impaired with regard to learning the new platform location, showing no preference for the training quadrant over the other quadrants (Figure 7D). Thus, although TMZ did not affect the ability of mice to learn the initial platform location, it blocked metformin's ability to promote enhanced learning on the reversal task.

To ensure that the TMZ regimen decreased the proportion of proliferating precursors in the hippocampus, we injected a subset of mice with BrdU immediately after the reversal task probe test. Analysis of hippocampi 24 hr later demonstrated that metformin/TMZ-treated mice had only approximately half as many BrdU-positive cells as did metformin/vehicle-treated mice (Figure 7J), confirming the efficacy of this treatment regime. Thus, inhibition of adult neurogenesis impairs metformin's ability to enhance spatial learning.

DISCUSSION

The findings presented here demonstrate that the widely used diabetes drug metformin is sufficient to activate the aPKC-CBP pathway in neural precursors and to thereby enhance neurogenesis and raise the possibility that metformin could provide the basis for a therapeutic strategy for the human nervous system. Specifically, these findings support five major conclusions. First, this work demonstrates that aPKCs ζ and ι play essential but distinct roles in regulating the genesis of neurons from radial precursors during embryonic development. aPKCζ regulates the differentiation of radial precursors into neurons by activating CBP, whereas aPKCι regulates the transition from radial precursors to basal progenitors, presumably by acting as part of the apical polarity complex (Costa et al., 2008). Second, by using a hESC-based approach for generating developing neural precursors, we show that aPKCs are also essential for human forebrain neurogenesis, at least in culture. Third, we show that metformin activates the aPKC-CBP pathway in neural precursors and that this activation promotes genesis of both human and rodent neurons in culture. Fourth, we show that metformin also promotes neurogenesis in the adult brain, enhancing the number of newly born neurons in both the olfactory bulb and the hippocampus. This adult neurogenesis requires CBP; when CBP is haploinsufficient, basal neurogenesis is unaffected, but metformin-induced neurogenesis is completely inhibited. Fifth, our behavioral studies demonstrate that metformin enhances spatial memory function coincident with a long-term increase in the number of newly born adult dentate gyrus neurons. When this metformin-induced neurogenesis is inhibited with the pharmacological agent TMZ, this also prevents the metformin-associated facilitation of spatial memory. Thus, metformin, by activating an aPKC-CBP pathway, recruits adult neural precursors and enhances neural function, thereby providing a candidate pharmacological approach for nervous system therapy.

There is considerable interest in the idea that recruitment of endogenous neural stem cells might provide a therapeutic strategy, based upon two lines of investigation. First, it is now clear that newly born adult neurons play a key role in the functionality of both the olfactory system and the hippocampus (Zhao et al., 2008). These findings are particularly relevant with regard to the hippocampus, because this structure plays a key role in normal cognition and is preferentially vulnerable in disorders such as ischemic stroke and Alzheimer's disease. Second, growing evidence indicates that adult neural stem cells are recruited in the injured and degenerating brain and that this represents an attempt at endogenous repair. Although the functional importance of this recruitment is still an open question, it is clear

that adult neural stem cells generate new neurons and oligodendrocytes in a number of neural injury paradigms (reviewed in Kernie and Parent, 2010), raising the hope that if this response could be enhanced, then perhaps it would promote repair. However, clinical approaches for recruiting adult neural stem cells in humans are currently lacking.

The search for pharmacological agents that can activate endogenous adult stem cells has led to a number of recently published chemical screens (reviewed in Li et al., 2012). Here, we have taken a different approach; we have defined an aPKC-CBP signaling pathway that is important for neural precursor differentiation (Wang et al., 2010; data presented here) and then focused upon a widely used drug, metformin, that activates this pathway in liver cells (He et al., 2009). In this regard, our data indicate that metformin does indeed activate the aPKC-CBP pathway to promote neurogenesis and that it coincidentally enhances hippocampus-dependent spatial memory formation, something that is thought to depend upon adult neurogenesis (Garthe et al., 2009). Equally importantly, we have shown that metformin has a similar activity on human neural precursors, increasing the likelihood that it might enhance neurogenesis in the human brain, as it does in the rodent.

Our findings also provide insights into the molecular mechanisms regulating neurogenesis. Our previous work demonstrated that CBP, a transcriptional coactivator and histone acetyltransferase, enhanced differentiation of developing radial precursors by binding to and acetylating genes that were important for neuronal and glial differentiation. This required CBP phosphorylation by aPKCζ, presumably when this kinase was itself activated in response to extrinsic stimuli. Here, we show that aPKCζ knockdown decreases neurogenesis and increases the maintenance of radial precursors. Moreover, we show that this phenotype can be rescued by expression of a CBP phosphomimic. Thus, activation of an aPKCζ-CBP pathway is essential for radial precursor differentiation, and our inhibition and knockdown studies indicate that metformin mediates its proneurogenic effects by activating this pathway. In contrast, for aPKCι, we show that it regulates neurogenesis but not gliogenesis in a CBP-independent fashion and that it enhances the transition from radial precursors to basal progenitors in vivo, thereby indicating a different role for this isoform. These findings are consistent with previous studies (Imai et al., 2006; Costa et al., 2008; Bultje et al., 2009) indicating that aPKCι is an essential component of an apical adherens/polarity complex that serves, in part, to maintain radial precursors. Thus, aPKCs ζ and ι play distinct and important roles in neural precursors.

Our in vivo studies demonstrate that metformin enhances neurogenesis in a CBP-dependent fashion in adult mice and our behavioral work suggests that the increase in hippocampal neurons is functionally relevant. In particular, we show that metformin preferentially enhances the reversal phase of the water maze task, and our data using TMZ to pharmacologically deplete adult precursors suggests that it does so by promoting genesis of new hippocampal neurons. In this regard, the specificity of the behavioral response is intriguing, because it raises the possibility that the initial acquisition of a spatial memory might have a somewhat different underlying neural substrate than the acquisition of a second, related spatial memory, with the latter involving newborn neurons.

Metformin is widely used in humans as a treatment for type II diabetes and other metabolic disorders. Intriguingly, there is widespread interest in using metformin in individuals with early-stage Alzheimer's disease because an increasing proportion of these individuals are also diabetic, and hyperinsulinemia may enhance the onset and progression of neurodegeneration. In this regard, a recent retrospective study indirectly suggested that metformin might improve some of the adverse neuroanatomical outcomes associated with AD (Beeri et al., 2008). Moreover, metformin has been shown to increase lifespan and delay the onset of cognitive impairment in a mouse model of Huntington's disease (Ma et al., 2007). Thus, while metformin may have other actions in the nervous system, our findings raise the possibility that its ability to enhance neurogenesis might have a positive impact in at least some nervous system disorders.

EXPERIMENTAL PROCEDURES

Animals

All animal use was approved by the Animal Care Committee of the Hospital for Sick Children in accordance with the Canadian Council of Animal Care policies. CD1 and C57BL/6 mice were obtained from Charles River Laboratory. C57/129J mice, which were used for the behavioral tests, were bred at the Hospital for Sick Children. All mice were maintained on a 12 hr light/12 hr dark cycle with ad libitum access to food and water. Mice were used at 2 months of age unless indicated otherwise, and behavioral procedures were conducted during the light phase of the cycle. B6.126S6-Crebbp^{tm1Dli} mice (*cbp*$^{+/-}$ mice) were obtained from The Jackson Laboratory and maintained as described (Wang et al., 2010).

Cell Culture Analysis

E11.5–E12.5 cortical precursors were isolated from CD1 embryos and cultured, transfected, and immunostained as described (Wang et al., 2010; Supplemental Information) at a plating density of 150,000–180,000 cells/ml. CNTF (50 ng/ml; Cedarlane Laboratories) and neuregulin-β (100 ng/ml; R&D Systems) were added 1 day after plating. Myristoylated aPKC peptide (2 μM; Calbiochem) and metformin (Sigma-Aldrich) were used as indicated. For quantification, more than 400 cells per condition in at least 8 randomly chosen fields per experiment were counted. Primary adult SVZ neurospheres were cultured as described (Fujitani et al., 2010). HEK293 cells were grown and transfected as described (Fujitani et al., 2010; Supplemental Information).

In Utero Electroporation

In utero electroporations and immunostaining were performed as described (Wang et al., 2010) with E13/E14 CD1 mice. For quantification, three to four fields per coronal section from each of four anatomically matched sections per brain were analyzed on a Zeiss Pascal confocal microscope, as previously described (Wang et al., 2010). A mean of four scans taken with a 40× objective were computed for each image.

Maintenance and Differentiation of hESCs

Undifferentiated HES2 cells were maintained in hESC medium as described (Kennedy et al., 2007) and prior to neural differentiation were depleted of feeder cells by culturing on Matrigel (BD Biosciences)-coated plates for 24 to 48 hr. Neuralized embryoid bodies (EBs) were generated by culturing small aggregates of feeder-depleted hESCs in low cluster plates (Corning Inc.) in knockout DMEM, supplemented with penicillin/streptomycin, 2 mM glutamine, 4 mM monothioglycerol, 50 μg/ml ascorbic acid (Sigma Aldrich), 5% N2 supplement (GIBCO), 5% B27 (GIBCO), and 20 ng/ml hbFGF at 37°C in an environment of 5% CO_2, 5% O_2, and 90% N2 for 24 hr. EBs were harvested, washed, and cultured in the same medium with 2 μM Dorsomorphin and 10 μM SB43152 for a further 12 days and then gently dissociated and plated on poly-d-lysine/laminin-coated plates in the same medium plus 20 ng/ml bhFGF,

10% N2 supplement, and 5% B27 supplement for 10 more days. For quantification, an average of 700 cells was counted per condition in 5–6 random fields per independent experiment.

BrdU Labeling

Mice were treated with BrdU (Sigma-Aldrich) as described for the SVZ (Morshead et al., 1998) and the hippocampus (Fujitani et al., 2010; Supplemental Information). For the hippocampus and main olfactory bulb, every tenth section was immunostained and quantitatively analyzed as described (Wojtowicz and Kee, 2006; Fujitani et al., 2010) and counts were normalized by multiplying for the total number of sections. For the SVZ, we quantified all cells within two to three cell diameters of the ventricular surface from four anatomically matched coronal sections from each animal.

Statistics

Statistical analyses were performed with a two-tailed Student's t test or ANOVA with Tukey's multiple comparison post hoc analysis, unless otherwise indicated. Error bars indicate the standard error of the mean (SEM).

Western Blot Analysis and Densitometry

Western blots were performed as previously described (Wang et al., 2010). Antibodies are in Supplemental Information. Densitometry was performed with Adobe (San Jose, CA) Photoshop.

Morris Water Maze

Two-month-old female C57/129J mice were used for all analyses and were injected daily with metformin (200 mg/kg) or sterile saline for the entirety of the experiment (Figure 7A). Some mice were also injected with 25 mg/kg TMZ or 10% DMSO as indicated (n = 28 sterile saline alone, n = 14 metformin alone, n = 14 metformin plus DMSO, and n = 13 metformin plus TMZ). Some were also injected with BrdU as indicated. Mice were trained on the hidden platform version of the water maze using a circular tank (120 cm diameter, 50 cm depth, 28°C) filled with 40 cm of water made opaque with nontoxic white paint. All testing was conducted under dim light. Extramaze visual cues were located on curtains surrounding the maze. The escape platform (10 cm diameter) was submerged 0.5 cm below the water surface. Acquisition was measured as latency to reach the platform and four possible start locations were pseudorandomly assigned to each trial. Actimetrics tracking software was used to record escape latency, swim speed, and distance traveled. Each animal was given three 60 s trials to find the platform with a 15 s intertrial interval across 5 days. After 5 days of training, mice were administered immediate (1 day) and remote (1 week) memory probe tests where the platform was removed and they searched for 60 s. Immediately after these tests, the platform was moved to the opposite location and animals were trained in the same manner for 2 additional days. The day after this reversal training, mice were given a probe test where the platform was removed and the amount of time spent searching in each quadrant was measured.

SUPPLEMENTAL INFORMATION

Supplemental Information includes Supplemental Experimental Procedures and five figures and can be found with this article online at doi:10.1016/j.stem.2012.03.016.

ACKNOWLEDGMENTS

The authors would like to thank Dennis Aquino, Sibel Naska, and Mark Gagliardi for technical support, advice, and discussions and Fred Wondisford for valuable insights and support. J.W. was supported by fellowships from the Multiple Sclerosis Society of Canada and the Three to Be Foundation, D.G. by a McEwen Center McMurrich fellowship, L.M.D. by an Alzheimer Society of Canada fellowship, G.I.C. by a Heart and Stroke Foundation of Canada fellowship, and D.T. by a CIHR Michael Smith studentship. P.W.F., D.R.K., and F.D.M. are Canada Research Chairs. This work was supported by funding from the CIHR (MOP86762 and MOP13958), the McEwen Center for Regenerative Medicine, the Canadian Stem Cell Network, and the Three to Be Foundation.

Received: February 8, 2011
Revised: March 9, 2012
Accepted: March 29, 2012
Published: July 5, 2012

REFERENCES

Alarcón, J.M., Malleret, G., Touzani, K., Vronskaya, S., Ishii, S., Kandel, E.R., and Barco, A. (2004). Chromatin acetylation, memory, and LTP are impaired in CBP+/- mice: a model for the cognitive deficit in Rubinstein-Taybi syndrome and its amelioration. Neuron *42*, 947–959.

Beeri, M.S., Schmeidler, J., Silverman, J.M., Gandy, S., Wysocki, M., Hannigan, C.M., Purohit, D.P., Lesser, G., Grossman, H.T., and Haroutunian, V. (2008). Insulin in combination with other diabetes medication is associated with less Alzheimer neuropathology. Neurology *71*, 750–757.

Bibel, M., Richter, J., Lacroix, E., and Barde, Y.A. (2007). Generation of a defined and uniform population of CNS progenitors and neurons from mouse embryonic stem cells. Nat. Protoc. *2*, 1034–1043.

Bultje, R.S., Castaneda-Castellanos, D.R., Jan, L.Y., Jan, Y.N., Kriegstein, A.R., and Shi, S.H. (2009). Mammalian Par3 regulates progenitor cell asymmetric division via notch signaling in the developing neocortex. Neuron *63*, 189–202.

Chambers, S.M., Fasano, C.A., Papapetrou, E.P., Tomishima, M., Sadelain, M., and Studer, L. (2009). Highly efficient neural conversion of human ES and iPS cells by dual inhibition of SMAD signaling. Nat. Biotechnol. *27*, 275–280.

Costa, M.R., Wen, G., Lepier, A., Schroeder, T., and Götz, M. (2008). Par-complex proteins promote proliferative progenitor divisions in the developing mouse cerebral cortex. Development *135*, 11–22.

Dupret, D., Fabre, A., Döbrössy, M.D., Panatier, A., Rodríguez, J.J., Lamarque, S., Lemaire, V., Oliet, S.H., Piazza, P.V., and Abrous, D.N. (2007). Spatial learning depends on both the addition and removal of new hippocampal neurons. PLoS Biol. *5*, e214.

Fujitani, M., Cancino, G.I., Dugani, C.B., Weaver, I.C., Gauthier-Fisher, A., Paquin, A., Mak, T.W., Wojtowicz, M.J., Miller, F.D., and Kaplan, D.R. (2010). TAp73 acts via the bHLH Hey2 to promote long-term maintenance of neural precursors. Curr. Biol. *20*, 2058–2065.

Garthe, A., Behr, J., and Kempermann, G. (2009). Adult-generated hippocampal neurons allow the flexible use of spatially precise learning strategies. PLoS ONE *4*, e5464.

He, L., Sabet, A., Djedjos, S., Miller, R., Sun, X., Hussain, M.A., Radovick, S., and Wondisford, F.E. (2009). Metformin and insulin suppress hepatic gluconeogenesis through phosphorylation of CREB binding protein. Cell *137*, 635–646.

Imai, F., Hirai, S., Akimoto, K., Koyama, H., Miyata, T., Ogawa, M., Noguchi, S., Sasaoka, T., Noda, T., and Ohno, S. (2006). Inactivation of aPKClambda results in the loss of adherens junctions in neuroepithelial cells without affecting neurogenesis in mouse neocortex. Development *133*, 1735–1744.

Kennedy, M., D'Souza, S.L., Lynch-Kattman, M., Schwantz, S., and Keller, G. (2007). Development of the hemangioblast defines the onset of hematopoiesis in human ES cell differentiation cultures. Blood *109*, 2679–2687.

Kernie, S.G., and Parent, J.M. (2010). Forebrain neurogenesis after focal Ischemic and traumatic brain injury. Neurobiol. Dis. *37*, 267–274.

Kung, A.L., Rebel, V.I., Bronson, R.T., Ch'ng, L.E., Sieff, C.A., Livingston, D.M., and Yao, T.P. (2000). Gene dose-dependent control of hematopoiesis and hematologic tumor suppression by CBP. Genes Dev. *14*, 272–277.

Li, W., Jiang, K., and Ding, S. (2012). Concise review: A chemical approach to control cell fate and function. Stem Cells *30*, 61–68.

Lopez-Atalaya, J.P., Ciccarelli, A., Viosca, J., Valor, L.M., Jimenez-Minchan, M., Canals, S., Giustetto, M., and Barco, A. (2011). CBP is required for environmental enrichment-induced neurogenesis and cognitive enhancement. EMBO J. *30*, 4287–4298.

Ma, T.C., Buescher, J.L., Oatis, B., Funk, J.A., Nash, A.J., Carrier, R.L., and Hoyt, K.R. (2007). Metformin therapy in a transgenic mouse model of Huntington's disease. Neurosci. Lett. *411*, 98–103.

Merkle, F.T., Tramontin, A.D., García-Verdugo, J.M., and Alvarez-Buylla, A. (2004). Radial glia give rise to adult neural stem cells in the subventricular zone. Proc. Natl. Acad. Sci. USA *101*, 17528–17532.

Messerschmidt, A., Macieira, S., Velarde, M., Bädeker, M., Benda, C., Jestel, A., Brandstetter, H., Neuefeind, T., and Blaesse, M. (2005). Crystal structure of the catalytic domain of human atypical protein kinase C-ι reveals interaction mode of phosphorylation site in turn motif. J. Mol. Biol. *352*, 918–931.

Miller, F.D., and Kaplan, D.R. (2012). Mobilizing endogenous stem cells for repair and regeneration: are we there yet? Cell Stem Cell *10*, 650–652.

Morshead, C.M., Craig, C.G., and van der Kooy, D. (1998). In vivo clonal analyses reveal the properties of endogenous neural stem cell proliferation in the adult mammalian forebrain. Development *125*, 2251–2261.

Naik, M.U., Benedikz, E., Hernandez, I., Libien, J., Hrabe, J., Valsamis, M., Dow-Edwards, D., Osman, M., and Sacktor, T.C. (2000). Distribution of protein kinase Mzeta and the complete protein kinase C isoform family in rat brain. J. Comp. Neurol. *426*, 243–258.

Oster, H., Eichele, G., and Leitges, M. (2004). Differential expression of atypical PKCs in the adult mouse brain. Brain Res. Mol. Brain Res. *127*, 79–88.

Stone, S.S., Teixeira, C.M., Devito, L.M., Zaslavsky, K., Josselyn, S.A., Lozano, A.M., and Frankland, P.W. (2011). Stimulation of entorhinal cortex promotes adult neurogenesis and facilitates spatial memory. J. Neurosci. *31*, 13469–13484.

Wang, J., Weaver, I.C.G., Gauthier-Fisher, A.S., Wang, H., He, L., Yeomans, J., Wondisford, F., Kaplan, D.R., and Miller, F.D. (2010). CBP histone acetyltransferase activity regulates embryonic neural differentiation in the normal and Rubinstein-Taybi syndrome brain. Dev. Cell *18*, 114–125.

Wojtowicz, J.M., and Kee, N. (2006). BrdU assay for neurogenesis in rodents. Nat. Protoc. *1*, 1399–1405.

Zhao, C., Deng, W., and Gage, F.H. (2008). Mechanisms and functional implications of adult neurogenesis. Cell *132*, 645–660.

Zhou, J., Su, P., Li, D., Tsang, S., Duan, E., and Wang, F. (2010). High-efficiency induction of neural conversion in human ESCs and human induced pluripotent stem cells with a single chemical inhibitor of transforming growth factor beta superfamily receptors. Stem Cells *28*, 1741–1750.